Heliyon 10 (2024) e27212

Contents lists available at ScienceDirect

Heliyon

journal homepage: www.cell.com/heliyon

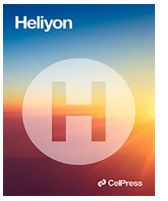

Research article

DNA methylation characteristics associated with chemotherapy resistance in epithelial ovarian cancer

Changling Duan [1], Zhongxin Yan [1], Cailiang Wu, Xuexin Zhou, Wei Bao [*]

Department of Obstetrics and Gynecology, Shanghai General Hospital, Shanghai Jiao Tong University School of Medicine, 200080, Shanghai, China

ARTICLE INFO

Keywords:
Methylation
Chemotherapy resistance
Ovarian cancer
DDR2
OPCML

ABSTRACT

Objective: The high mortality rate of epithelial ovarian cancer (EOC) is often attributed to the frequent development of chemoresistance. DNA methylation is a predictive biomarker for chemoresistance.

Methods: This study utilized DNA methylation profiles and relevant information from GEO and TCGA to identify different methylated CpG sites (DMCs) between chemoresistant and chemosensitive patients. Subsequently, we constructed chemoresistance risk models with DMCs. The genes corresponding to candidate DMCs in chemoresistance risk models were further analyzed to identify different methylated gene symbols (DMGs) associated with chemoresistance. The DMGs that showed a strong correlation with the corresponding DMCs were analyzed through immunohistochemistry.

Results: Compared to chemosensitive EOC patients, chemoresistant patients showed 423 hypermethylated CpGs and 1445 hypomethylated CpGs. The chemoresistance risk models based on DMCs have shown the improved predictive ability for chemoresistance in EOC (AUC = 65.0–76.2%). The methylations of cg25510164, cg13154880, cg15362155 and cg08665359 were strongly associated with decreased risk of chemoresistance. Conversely, the methylation of cg08872590 and cg14739437 significantly increased the risk. We identified 13 DMGs, from 47 DMCs corresponding genes, between chemosensitive and chemoresistant samples. Among the DMGs, the expression levels of DDR2 and OPCML exhibited strong correlations with the corresponding DMCs. DDR2 and OPCML both showed enhanced expression in chemoresistant ovarian microarray tissue.

Conclusions: Hypomethylated CpGs may play a significant role in DNA methylation associated with chemoresistance in EOC. The epigenetic modification of DDR2 could have important implications for the development of chemoresistance. Our study provides valuable insights for future research on DNA methylation in the chemoresistance of EOC.

1. Introduction

Ovarian cancer is a highly lethal gynecologic cancer and is the seventh most common cancer among women worldwide. The five-year survival rate after diagnosis is only 46% [1]. In developed countries, over 90% of malignant ovarian tumors originate from epithelial cells [2]. The standard treatment for patients with epithelial ovarian cancer (EOC) is surgical debulking with complete

* Corresponding author.
E-mail address: forever_chipper@hotmail.com (W. Bao).
[1] Contributed equally.

https://doi.org/10.1016/j.heliyon.2024.e27212
Received 22 February 2024; Accepted 26 February 2024
Available online 29 February 2024

cytoreduction, followed by platinum-based chemotherapy [3]. However, approximately 25% of patients with EOC exhibit resistance to chemotherapy treatments, and recurrences are also frequent among responders [4]. Patients with EOC have had little improvement in long-term survival over the last decades, while standard treatment remains platinum-based combination chemotherapy [5]. Therefore, it is crucial to identify a reliable method for predicting chemoresistance and developing new therapeutic strategies for EOC. However, there is a lack of accurate clinical biomarkers to predict chemoresistance in EOC. Deoxyribonucleic acid (DNA) methylation is the most studied epigenetic alteration and is regarded as one of the most stable gene-silencing mechanisms [6]. Hypermethylation of CpG islands (CpGs) in gene promoters leads to gene silencing, whereas hypomethylation is usually linked to gene expression [7]. It is reported that changes in DNA methylation have been associated with chemoresistance in ovarian cancer [8] and usually occur before the start of chemoresistance [9]. DNA methylation is chemically and biologically stable and can be measured in cell-free cancer DNA in the blood [10]. Furthermore, unlike genetic mutations, DNA methylation can be reversed. The sensitivity of ovarian cancer patients to chemotherapy can be improved by demethylation drugs [11,12]. Thus, the methylation of genes holds promise for its use as a predictive biomarker of chemoresistance and may represent a promising therapeutic target.

Recently, there have been more studies on DNA methylation and its relation to chemotherapy resistance in ovarian cancer, involving a larger number of genes [13]. However, the results of the relationship between chemotherapy resistance and epigenetic alterations are confusing and contradictory [14]. In this study, we analyze DNA methylation and ribonucleic acid (RNA) sequencing transcriptomics data, as well as clinical information from the Cancer Genome Atlas (TCGA, https://tcga-data.nci.nih.gov/tcga) database, and DNA methylation data from the Gene Expression Omnibus (GEO, http://www.ncbi.nlm.nih.gov/geo/) to investigate the methylation characteristics of chemotherapy resistance in EOC.

2. Materials and methods

2.1. Data acquisition

The DNA methylation profile of GSE65820 [15], which is based on the GPL13534 (Illumina HumanMethylation450 BeadChip, Illumina 450K) platform, was obtained from the GEO database. This dataset consists of 80 samples of high-grade serous ovarian cancer. We defined the chemoresistant samples as the patients whose disease had progressed within 6 months after the last platinum treatment, including 37 platinum-resistant and 12 refractory ovarian cancer samples in GSE65820 [15]. Another 31 samples were chemosensitive, whose disease had relapsed more than 6 months after platinum-based chemotherapy.

In addition, the methylation profile, RNA sequencing transcriptomics data and corresponding clinical information were retrieved for ovarian cancer from the TCGA database. There are 758 samples in the TCGA-OV dataset. Firstly, 177 samples without a primary therapy outcome were excluded. Subsequently, two samples with an overall survival (OS) time of less than 30 days were excluded. Finally, 480 out of 581 filtered samples contained methylation microarray data. The Illumina HumanMethylation27 BeadChip (Illumina 27K) microarray contained 41 chemoresistant and 434 chemosensitive samples. There were 1 chemoresistant and 4 chemosensitive samples based on Illumina 450K.

2.2. Screening of different methylated CpG sites (DMCs)

The raw data from GSE65820 [15] were transformed into β value [β = intensity of the methylated allele (M)/(intensity of the unmethylated allele (U) + intensity of the methylated allele (M) +100)] by R package *minfi*. The DMCs between chemoresistant and chemosensitive patients were identified using the R package *minfi* ($|\text{Delta Beta}|>0.08$, $P < 0.05$). Delta beta (Δβ) refers to the difference between the average β value of the chemoresistant group and the average β value of the chemosensitive group. The volcano plot and heatmap of DMCs were plotted and visualized with the R package *ggplot2* and *ComplexHeatmap*, respectively. Manhattan plot was built to show the distribution of DMCs by *CMplot* package in R. The specific distribution of DMCs on all chromosomes was shown by the R package *RIdeogram*. The corresponding genes of DMCs in GPL13534 were enriched in Gene Ontology (GO, http://geneontology.org/) and Kyoto Encyclopedia of Genes and Genomes (KEGG, http://www.genome.jp/kegg/) databases by R package *clusterProfiler*.

2.3. Construction and validation of chemoresistance prediction DMCs model

The DMCs between chemoresistant and chemosensitive patients in GSE65820 [15] were further analyzed to predict the chemoresistance of EOC through the methylation microarray data of TCGA. For samples derived from Illumina 27K, the association of the DMCs with chemoresistance was analyzed via univariate logistic regression analysis with $P < 0.05$ as the threshold. DMCs with a p-value less than 0.05 were chosen for subsequent multivariate logistic regression analysis to develop the chemoresistance risk model. The 475 samples were randomly assigned to either the training set (n = 333) or the validation set (n = 142). For the Illumina 450K samples, we divided 70% of samples of GSE65820 [15] (n = 57) into the training set, the remaining 23 samples and 5 samples from TCGA were assigned to the validation set. The least absolute shrinkage and selection operator (LASSO) regression was applied to identify the candidate DMCs and construct the chemoresistance risk model by R package *glmnet*. We used cross-validation to determine the lambda-min, which corresponds to the lowest deviance of the model. The receiver operating characteristic (ROC) curve was plotted via the R package *pROC* to assess the performance of the Illumina 27K and Illumina 450K chemoresistance risk models. The forest plot was generated to summarize the information of the candidate DMCs constructing Illumina 27K and Illumina 450K risk models through the R package *forestploter*.

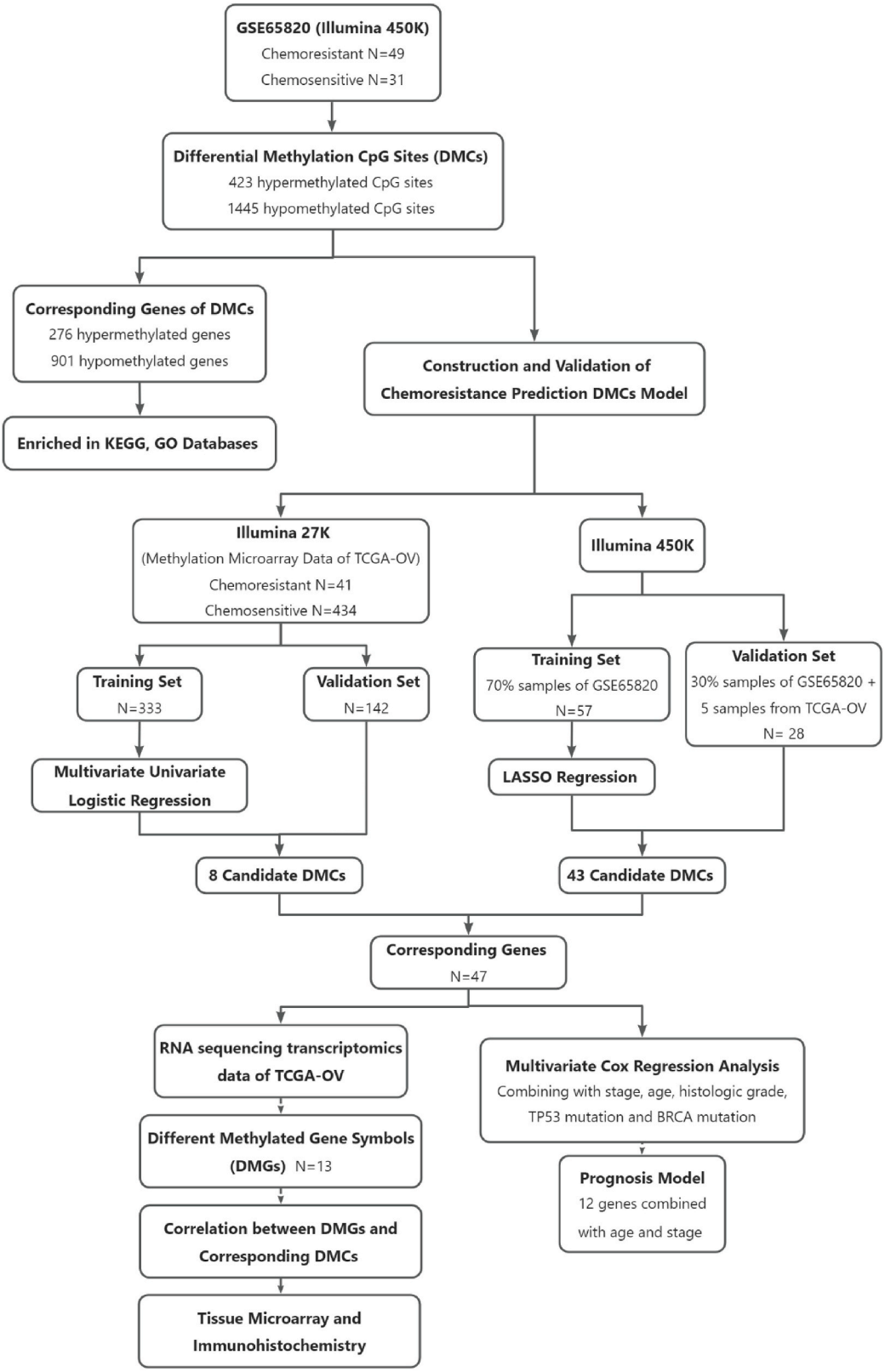

Fig. 1. The whole flow diagram of this study.

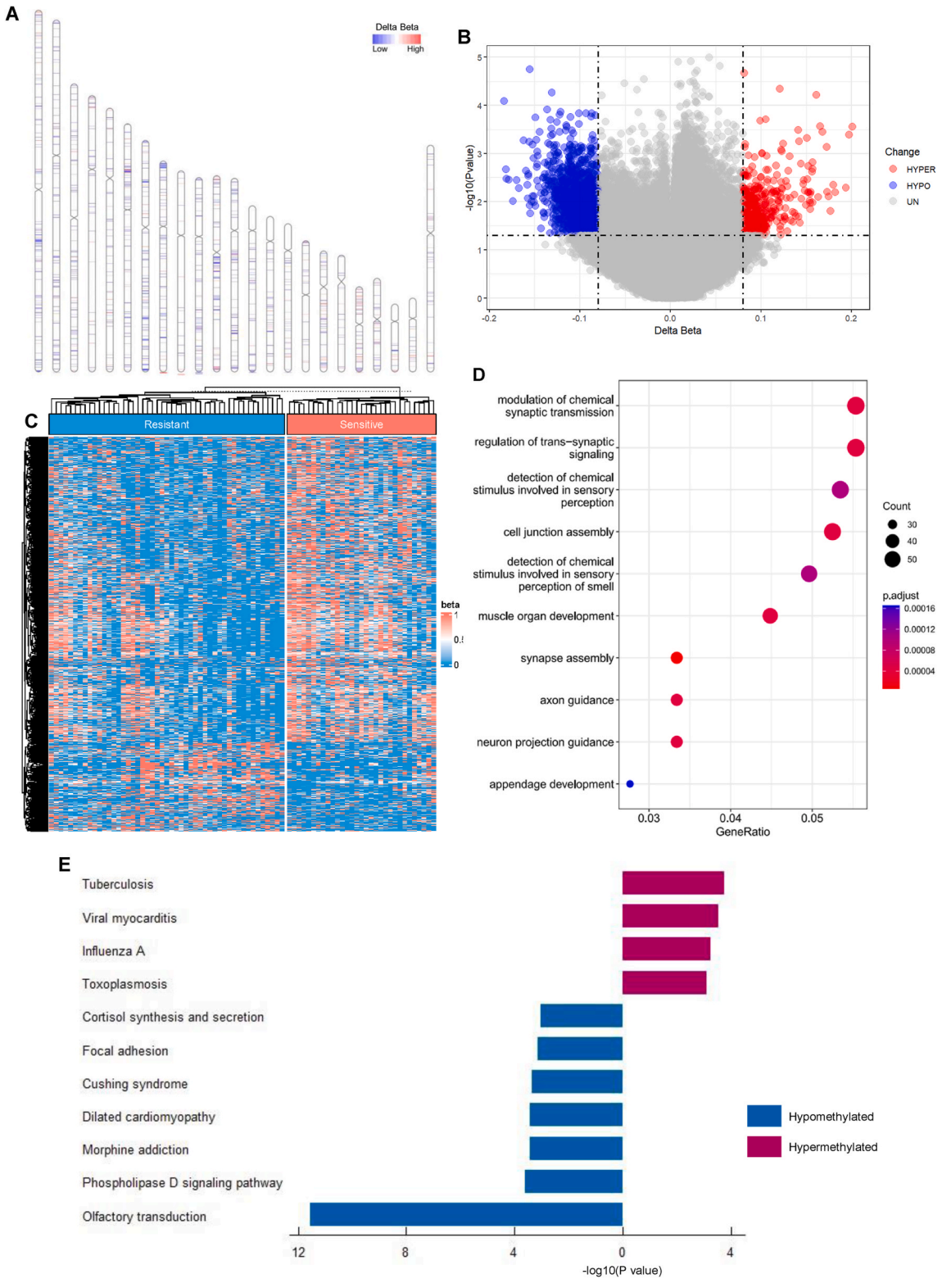

(caption on next page)

Fig. 2. (A) The distribution of DMCs on all chromosomes, the blue lines represent the hypomethylated DMCs and the red lines are hypermethylated DMCs. (B) The volcano plot of DMCs between chemoresistant and chemosensitive group. The x axis and y axis show delta beta and -log10(p-value) of CpGs between chemoresistant and chemosensitive group. The blue points represent the hypomethylated DMCs and the red points are hypermethylated DMCs, with the cutoff |Delta Beta|>0.08, $P < 0.05$. (C) The heatmap of DMCs. Row and column represented DMCs and tissue samples, respectively. The color scale represented the beta-values. (D) The top 10 significant enrichment GO terms of DMCs corresponding genes. The x axis shows gene ratio, the color means p values and the y axis shows GO terms. (E) The significant enrichment KEGG pathways of DMCs corresponding genes with $p < 0.001$. The x axis shows -log10(P value) and y axis shows KEGG pathways. The red bars represent hypermethylated genes corresponding pathways, blue means hypomethylated genes corresponding pathways. Delta Beta, the difference between the average β value of the chemoresistant group and the average β value of the chemosensitive group. (For interpretation of the references to color in this figure legend, the reader is referred to the Web version of this article.)

2.4. Prognosis model with the corresponding genes of candidate DMCs

To evaluate the effect of DMCs on survival outcome, the corresponding genes of candidate DMCs constituting chemoresistance prediction models based on the Illumina 27K and Illumina 450K were analyzed via Kaplan-Meier plot. Meanwhile, the corresponding genes were selected to construct the prognosis model through multivariate Cox regression analysis, combining with stage, age and histologic grade. In this step, the R packages *survminer* and *survival* were applied. The forest plot was generated to show the prognosis model using the R package *forestploter*. Using the median of the risk score as the cutoff point, the samples were divided into the high-risk group and the low-risk group. Subsequently, Kaplan–Meier plots were used to illustrate overall survival using the R packages *survival* and *survminer*. The ROC curve was plotted via the R package *timeROC* to evaluate the predictive capacity of this prognosis model for overall survival.

2.5. Correlation between different methylated gene symbols (DMGs) and corresponding DMCs

The corresponding genes of candidate DMCs constituting chemoresistance risk models based on the Illumina 27K and Illumina 450K were further analyzed with RNA sequencing transcriptomics data of TCGA ovarian cancer samples. The DMGs between chemoresistant and chemosensitive patients were confirmed by R package *DESeq2*. The volcano plot of DMGs was plotted and visualized with the R package *ggplot2*. The correlation between DMGs and corresponding DMCs was evaluated and plotted by R package *corrplot*. For DMGs and corresponding DMCs whose correlation coefficients were equal or greater than 0.5, the scatter diagram was drawn by R package *ggpubr*.

2.6. Tissue microarray and immunohistochemistry

Chemoresistant ($n = 20$) and chemosensitive ($n = 48$) tissue microarrays were procured from Shanghai Zuocheng Biotech (Shanghai, China). The immunohistochemistry analysis was performed as previously described [16]. The antibodies used in the study included anti-DDR2 rabbit monoclonal antibody (1:50, HA721479, Huaan Biotechnology), anti-HSPA1A rabbit polyclonal antibody (1:200, ER50802, Huaan Biotechnology), anti-OPCML rabbit polyclonal antibody (1:50, Bs-1081R, Bioss). The optical density (OD) was used to evaluate the expression level of each protein by the software *ImageJ*. The comparison and visualization of the difference in ODs between the chemoresistant group and chemosensitive group were conducted using the R package *ggpubr*.

2.7. Statistical analysis

All of the statistical processes and graph creation were conducted using the R software (version 4.3.0). The Wilcoxon test was used to compare the numerical values between the two groups. The Kaplan-Meier plot was carried out to present survival curves, and the log-rank test was applied to calculate the significance. Spearman analysis was used to investigate the correlation coefficient between DMGs and corresponding DMCs. For all the analyses above, $p < 0.05$ in the two-tailed test was considered statistically significant without the need for a formal declaration.

3. Results

3.1. DMCs between chemoresistant and chemosensitive patients

The whole flow diagram of this study is presented in Fig. 1. Originally, there were 448889 probes in the raw data of GSE65820 [15]. After filtration of invalid or duplicate probes, 407807 CpGs were described as β value. Subsequently, 1868 significant DMCs were identified between chemoresistant and chemosensitive EOC samples. Compared with chemosensitive patients, there were 423 hypermethylated CpGs (corresponding to 276 genes) and 1445 hypomethylated CpGs (corresponding to 901 genes) in chemoresistant patients. The distribution of DMCs on all chromosomes is shown in Fig. 2A and Fig. S1A. The majority of DMCs were located in the promoter or body of genes, as well as in the open sea of CpG islands (Figs. S1B–C). The volcano plot and heatmap were used for the visualization of DMCs between chemoresistant and chemosensitive groups (Fig. 2B–C). The signaling pathways of DMCs corresponding genes enriched in the KEGG database include olfactory transduction, phospholipase D signaling pathway, morphine addiction, cortisol synthesis and secretion, dilated cardiomyopathy, focal adhesion and infectious diseases. The GO enrichment analysis includes

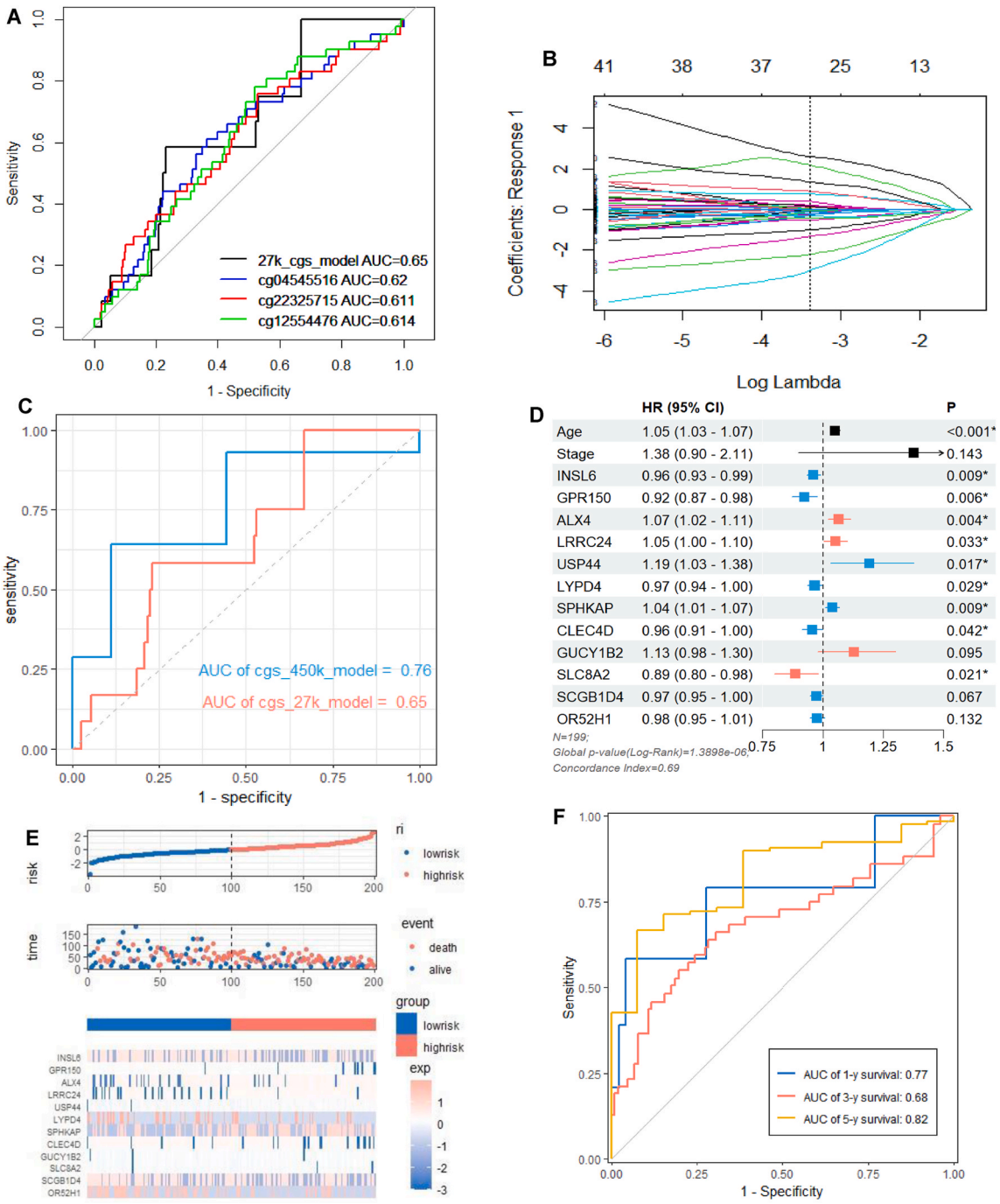

Fig. 3. (A) ROC curves of the chemoresistance risk model and candidate DMCs based on the Illumina 27K to predict chemotherapy sensitivity in ovarian cancer. Candidate DMCs with AUC>0.6 were showed in this figure.(B) The chemoresistance risk model based on the Illumina 450K was developed through LASSO regression with lambda min. The x axis shows different log lambda, the y axis shows the coefficients of DMCs to chemoresistance. The vertical dashed line represents log(lambda-min). (C) ROC curves of chemoresistance risk models constructed by DMCs in the Illumina 27K and Illumina 450K. (D) Forest plot of the multivariate Cox regression analysis results of prognostic model. Red lines and blocks represent hypermethylated CpGs corresponding genes, blue means hypomethylated CpGs corresponding genes. (E) The risk curve and scatter plot of samples in the TCGA-OV project ordered by the risk score of prognosis, and the heatmap of expression profiles of the genes constructing prognostic model. (F) The1-, 3- and 5-year ROC curves of the prognostic model. AUC, area under curve; ROC, receiver operating characteristic. *p < 0.05. (For interpretation of the references to color in this figure legend, the reader is referred to the Web version of this article.)

Probes	Symbols	Methylation	Regions	OR (95% CI)	P
cg04545516	SEMG1	HYPO	Body	0.17 (0.04 - 0.67)	0.01139
cg11830061	INSL6	HYPO	1stExon	0.13 (0.02 - 0.67)	0.01499
cg18841634	DCC	HYPO	Body	0.01 (0.00 - 0.80)	0.03955
cg00850538	CRIM1	HYPO	Promoter	0.26 (0.07 - 0.95)	0.04205
cg02620013	MLNR	HYPO	1stExon	0.18 (0.03 - 1.00)	0.04996
cg07924575	HPS4	HYPO	Promoter	0.19 (0.04 - 0.98)	0.04755
cg22325715	CNTD1	HYPO	Promoter	0.22 (0.06 - 0.75)	0.01556
cg12554476	GP2	HYPO	Promoter	0.25 (0.08 - 0.78)	0.01700
cg07180458	AKR7L	HYPER	Promoter	39.23 (1.98 - 778.31)	0.01607
cg06921573	DMRTA2	HYPO	Promoter	0.00 (0.00 - 0.10)	0.00391
cg23028772	DDR2	HYPO	Promoter	0.02 (0.00 - 0.32)	0.00614
cg04836492	OR2T11	HYPO	Promoter	0.01 (0.00 - 0.26)	0.00644
cg12565502	SPHKAP	HYPO	Body	0.00 (0.00 - 0.05)	0.00191
cg15626105	ABI3BP	HYPO	Body	0.00 (0.00 - 0.26)	0.00951
cg25510164	**GBA3**	**HYPO**	**Body**	**0.00 (0.00 - 0.05)**	**0.00035**
cg00967552	SLC10A4	HYPO	Body	0.01 (0.00 - 0.24)	0.00467
cg13154880	**SLC10A4**	**HYPO**	**Body**	**0.00 (0.00 - 0.06)**	**0.00076**
cg22736323	PDGFRA	HYPO	Promoter	0.38 (0.04 - 3.95)	0.41605
cg26472636	SDHAP3	HYPER	Body	37.78 (1.31 - 1088.92)	0.03420
cg18035255	OTP	HYPO	Body	0.00 (0.00 - 0.05)	0.00163
cg26224060	GPR150	HYPO	1stExon	0.02 (0.00 - 0.30)	0.00499
cg21137557	LVRN	HYPER	Body	232.90 (3.56 - 15239.84)	0.01062
cg12883479	HSPA1A	HYPER	Promoter	10.58 (1.91 - 58.62)	0.00693
cg15398520	LPAL2	HYPO	Promoter	0.95 (0.27 - 3.35)	0.93491
cg09349530	TBX20	HYPO	Promoter	0.02 (0.00 - 0.50)	0.01850
cg08872590	**LRRC24**	**HYPER**	**Body**	**162.10 (8.71 - 3015.02)**	**0.00065**
cg14739437	**LRRC24**	**HYPER**	**Body**	**182596.42 (186.80 - 178487953.97)**	**0.00056**
cg26333393	CPXM2	HYPO	Promoter	0.00 (0.00 - 0.32)	0.01514
cg24561952	OR52H1	HYPO	Promoter	0.00 (0.00 - 0.06)	0.00149
cg14707162	PLEKHA7	HYPO	Promoter	0.03 (0.00 - 0.52)	0.01697
cg06245037	ALX4	HYPER	Promoter	16.46 (1.14 - 237.97)	0.03986
cg15362155	**SCGB1D4**	**HYPO**	**Promoter**	**0.00 (0.00 - 0.03)**	**0.00091**
cg06967998	OPCML	HYPER	Body	807.88 (13.70 - 47657.96)	0.00129
cg05035315	OPCML	HYPER	Body	844.62 (7.30 - 97778.56)	0.00544
cg11349423	OPCML	HYPO	Body	0.01 (0.00 - 0.42)	0.01697
cg01253753	CLEC4D	HYPO	Promoter	0.00 (0.00 - 0.08)	0.00292
cg00927554	USP44	HYPO	Promoter	0.03 (0.00 - 0.48)	0.01369
cg27066989	GUCY1B2	HYPER	Promoter	32.65 (2.11 - 505.45)	0.01264
cg04398180	ADPRHL1	HYPER	Promoter	16.39 (1.52 - 176.32)	0.02103
cg16319578	HSPA2	HYPER	Promoter	1.15 (0.36 - 3.70)	0.81397
cg04223832	MIR655	HYPER	Promoter	25.11 (1.32 - 476.68)	0.03188
cg00215587	MKRN3	HYPO	Promoter	0.00 (0.00 - 0.16)	0.00315
cg17794320	KIF7	HYPER	Body	133.16 (5.32 - 3330.80)	0.00290
cg11849132	LYPD4	HYPO	Promoter	0.00 (0.00 - 0.04)	0.00612
cg07516091	SLC8A2	HYPER	Body	16.36 (1.11 - 241.25)	0.04175
cg11749672	CD37	HYPER	Body	19.60 (1.17 - 327.21)	0.03829
cg08665359	**EBF4**	**HYPO**	**Body**	**0.00 (0.00 - 0.01)**	**0.00082**
cg07378350	GDF5	HYPER	Promoter	0.31 (0.08 - 1.17)	0.08314
cg13353337	LZTR1	HYPER	Promoter	139.82 (5.79 - 3373.91)	0.00235
cg01821005	MAGEB1	HYPER	Promoter	213.91 (4.62 - 9907.70)	0.00611
cg07368951	SPIN4	HYPO	Promoter	0.00 (0.00 - 0.04)	0.00108

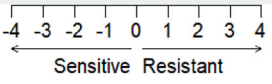

(caption on next page)

Fig. 4. The forest plot of the univariate Logistic regression analyses results of all 51 candidate DMCs constructing chemoresistance risk model and their corresponding information. The red lines represent hypermethylated CpGs and blue means hypomethylated CpGs. For better presentation, ORs and 95%CIs were calculated to log10 (OR) and log10 (95%CI) in this plot. (For interpretation of the references to color in this figure legend, the reader is referred to the Web version of this article.)

processes such as appendage development, muscle organ development, cell junction assembly, and regulation of signalings in the nervous system.(Fig. 2D–E).

3.2. The ability of DMCs to predict chemoresistance in ovarian cancer

In ovarian cancer samples from TCGA, there were no significant differences in age, grade and stage between the chemoresistant and chemosensitive groups. The R0 surgical debulking in chemoresistant patients was significantly less than in chemosensitive patients (Table S1). The 1868 DMCs between chemoresistant and chemosensitive patients in GSE65820 [15] based on Illumina 450K remained 142 in the Illumina 27K, including 37 hypermethylated CpG sites and 105 hypomethylated CpG sites. The univariate logistic regression analysis revealed 8 candidate DMCs that were significantly associated with chemoresistance. These DMCs were identified as "cg04545516", "cg11830061", "cg18841634", "cg00850538", "cg02620013", "cg07924575", "cg22325715", and "cg12554476". Then, the 8 candidate DMCs were utilized to establish a chemoresistance risk model through multivariate logistic regression analysis in the training set. The risk score was calculated as follows: Risk score = $-0.50955 \times$ cg04545516–$0.42954 \times$ cg11830061–$0.08763 \times$ cg18841634 + $0.36330 \times$ cg00850538 – $0.06725 \times$ cg02620013 + $0.13689 \times$ cg07924575 + $0.172 \times$ cg22325715–$0.27279 \times$ cg12554476. ROC analysis was performed to analyze the predicted value. The sensitivity, specificity and area under the curve (AUC) of 8 candidate CpGs methylation to predict chemotherapy sensitivity were 56.1–95.1%, 27.6–67.1% and 0.570–0.62(Fig. 3A and Figs. S2A–E). The sensitivity, specificity and AUC of the chemoresistance risk model were 58.3%, 76.9% and 0.650 (Fig. 3A).

There were only 10 ovarian cancer samples based on Illumina 450K in TCGA, including 1 chemoresistant and 4 chemosensitive samples. 70% samples of GSE65820 [15] (n = 57) contained 35 chemoresistant and 22 chemosensitive samples were assigned to the training set. The chemoresistance risk model was developed through LASSO regression (Fig. 3B). We applied lambda min (0.03396805) to select 43 candidate DMCs (Fig. S2F). The sensitivity, specificity and AUC of the chemoresistance risk model were 64.3%, 88.9% and 0.762 (Fig. 3C).

All candidate DMCs were analyzed by univariate logistic regression analysis, the results and corresponding information were summarized in Fig. 4. Among the candidate DMCs, the methylation of cg25510164, cg13154880, cg15362155, and cg08665359 showed strong effects in reducing the risk of chemoresistance ($p < 0.001$). Corresponding to the expression of genes GBA3, SLC10A4, SCGB1D4, and EBF4. The cg08872590 and cg14739437, corresponding to the expression of genes LRRC24, were significantly related to increasing the risk of chemoresistance.

In the 47 corresponding genes of candidate DMCs, the multivariate Cox regression analysis selected 12 genes including INSL6, GPR150, ALX4, LRRC24, USP44, LYPD4, SPHKAP, CLEC4D, GUCY1B2, SLC8A2, SCGB1D, OR52H1 combined with age and stage to set up a prognostic model (Fig. 3D). Among the 12 genes, the expressions of INSL6, GPR150, LYPD4, CLEC4D, SLC8A2, SCGB1D and OR52H1 decreased, while that of ALX4, LRRC24, USP44, SPHKAP and GUCY1B2 relatively improved the survival outcomes in ovarian cancer. The patients were classified into high-risk and low-risk groups according to the median of the risk. The risk score, survival outcome and expression of selected genes of patients in the two subgroups are shown in Fig. 3E and Fig. S2G. The time-dependent ROC curve indicated that the risk score had relatively higher accuracy in predicting the 1-year (AUC = 0.77) and 5-year OS (AUC = 0.82) (Fig. 3F).

3.3. Correlation between DMGs and corresponding DMCs

In RNA sequencing transcriptomics data of TCGA ovarian cancer samples, the 47 corresponding genes of 51 candidate DMCs were further analyzed with chemoresistance. We found 13 DMGs between chemosensitive and chemoresistant samples, including 4 upregulated and 9 downregulated genes (Fig. 5A). 2 genes were excluded as incomplete information of methylation probes. We found that among the 11 DMGs and 14 corresponding DMCs, the expression of DMGs was mainly negatively correlated with methylation levels of DMCs (Fig. 5B). HSPA1A was significantly negatively correlated with corresponding DMC cg12883479 ($R = -0.82$, $p = 0.034$, Fig. 5C). Besides, DDR2, ADPRHL1, MAGEB1, and DMRTA2 showed negative correlation with corresponding DMCs cg04398180, cg01821005, cg06921573 and cg23028772, respectively ($R = -0.63 \sim -0.5$, $p = 0.13–0.27$, Fig. 5D and Fig. S3). OPCML showed a positive correlation with corresponding DMC cg05035315 ($R = 0.67$, $p = 0.1$, Fig. 5E).

3.4. Expression of HSPA1A, DDR2 and OPCML in EOC

The expression of HSPA1A, DDR2 and OPCML is significantly correlated with the corresponding DMCs. The possible physiological role of HSPA1A, DDR2 and OPCML has been reported. We further validated their expression differences in tumor microarrays to explore the potential epigenetic alterations related to chemoresistance. We summarized and conducted differential analyses for age, histotype, grade, stage and survival outcomes of tumor microarrays (Table S2). There are no differences in the clinical characteristics between the chemoresistant and chemosensitive groups. The expression of HSPA1A, DDR2 and OPCML in EOC was studied by immunohistochemistry. In the tissue array composed of 68 ECO patient samples, immunohistochemistry revealed that the OD of DDR2

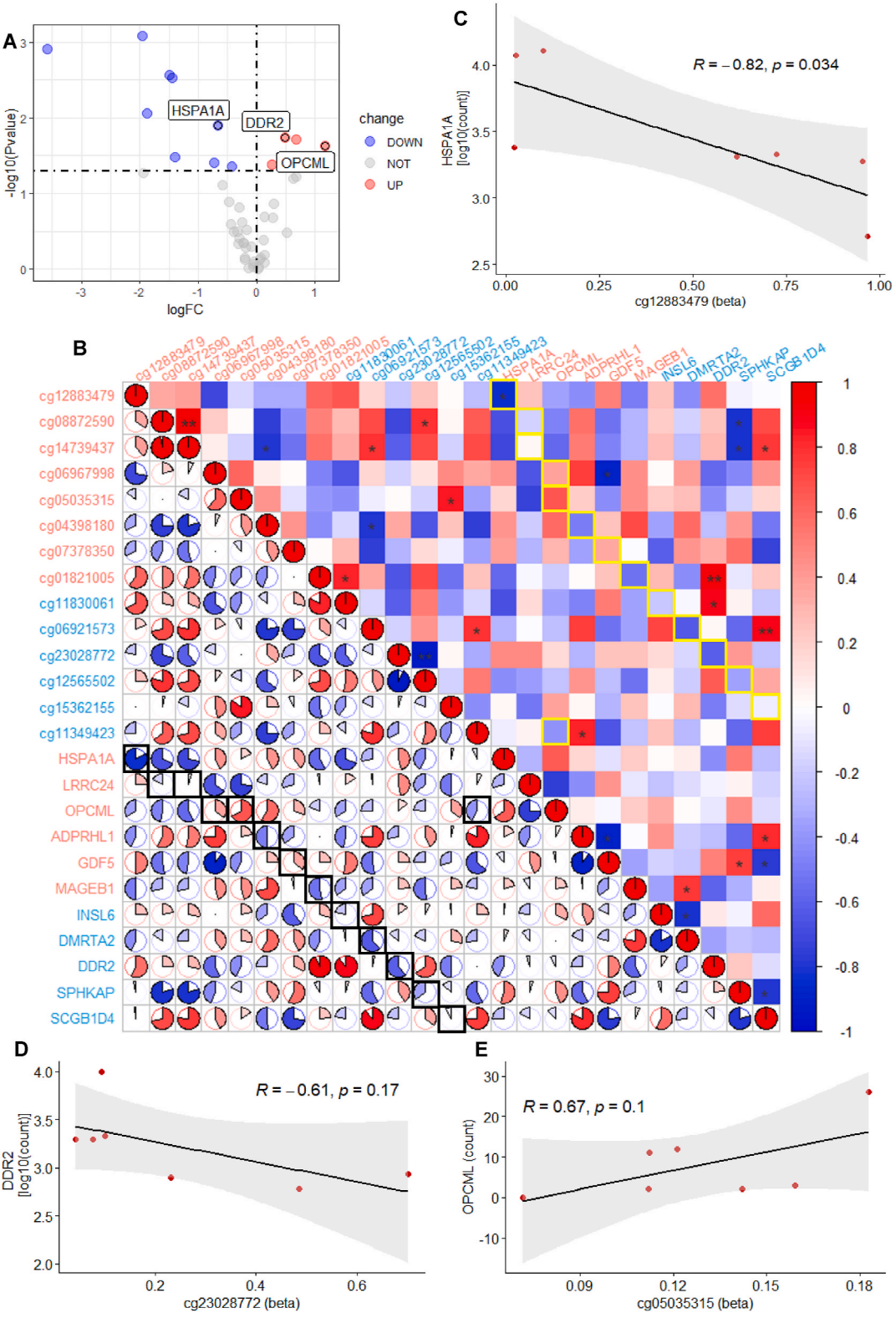

(caption on next page)

Fig. 5. (A) The volcano plot of 13 DMGs between chemosensitive and chem oresistant samples. The x axis and y axis show logFC and -log10(p-value) of DMGs. (B) Heatmap showing the correlation between 13 DMGs and corresponding DMCs. The block with a black or yellow border means the correlation result between the DMG and its corresponding DMC. Red names represent hypermethylated DMGs and DMCs, blue names are hypomethylated DMGs and DMCs. Red block and pie mean in positive relation, while blue represents the negative. *$p < 0.05$; **$p < 0.01$. (C–E) The relationship between expression of HSPA1A, DDR2, OPCML and methylation of corresponding CpG. C.cg12883479 methylation and HSPA1A expression. D. cg23028772 methylation and DDR2 expression. E.cg05035315 methylation and OPCML expression. (For interpretation of the references to color in this figure legend, the reader is referred to the Web version of this article.)

and OPCML in chemoresistant ovarian tissue was higher than that of chemosensitive ($p = 0.0024$, $p = 0.024$, respectively) (Fig. 6A–B). DDR2 was mainly expressed in the cytoplasm (Fig. 6A). In chemosensitive tissue, OPCML was negative in the ovarian interstitial cell. However, OPCML was expressed in all ovarian cells of chemoresistant tissue, both nucleus and cytoplasm (Fig. 6B). HSPA1A was expressed both in the nucleus and cytoplasm, with no statistical difference observed between chemoresistant and chemosensitive patients ($P = 0.74$) (Fig. 6C).

4. Discussions

In the present study, we used methylation microarray data obtained from TCGA and GEO to identify the DMCs associated with chemoresistance in patients with EOC. Our results indicate that DMCs are predominantly hypomethylated in chemoresistant EOC

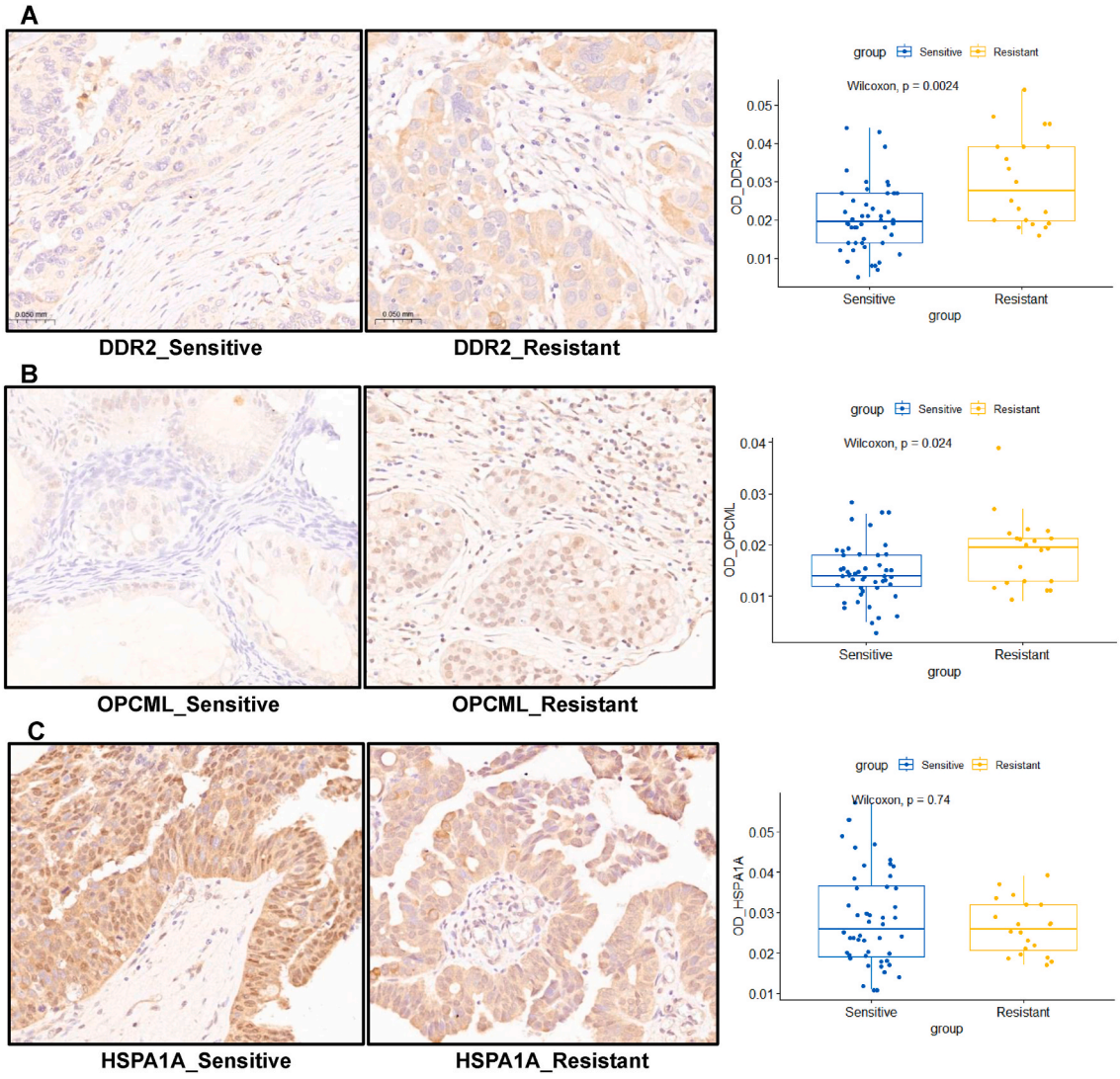

Fig. 6. (A–C) The immunohistochemical stain (40 ×) and OD of DDR2, OPCML and HSPA1A in chemosensitive and chemoresistant EOC tissue. OD, optical density.

patients. The chemoresistance risk models based on the Illumina 27K and 450K platforms have demonstrated promising predictive capabilities for identifying chemoresistance in EOC. Additionally, the corresponding genes of candidate DMCs also showed prognostic value. Among the DMGs, the expression of DDR2 and OPCML in chemoresistant ovarian tissue was found to be higher than that of chemosensitive, which also showed a strong correlation with corresponding DMCs.

4.1. DNA methylation changes associated with chemoresistant in EOC

DNA methylation is the most studied epigenetic alteration [14]. Hypermethylation of CpGs in gene promoters leads to gene silencing, while hypomethylation is usually linked to gene expression [7]. Some studies have shown that gene-body methylation, in addition to promoter methylation, can also impact gene expression [17]. Our results indicate that the majority of DMCs were located in the promoter and body of genes. It has been reported that hypermethylation is the primary form of methylation observed in platinum-resistant ovarian cancer cell lines [18]. Results from preclinical and early-stage clinical studies suggest that DNA hypomethylation drugs, such as DNA methyltransferase inhibitors (DNMTi) may have the potential to reverse chemoresistance [19,20]. In this study, we discovered that DMCs are predominantly hypomethylated in chemoresistant EOC patients. Hypomethylation drugs such as DNMTi may need to be used cautiously due to the potential to increase the risk of chemoresistance. Targeted methylation of specific genes may represent an alternative strategy to enhance chemotherapy sensitivity in EOC [21]. Ideally, in the future, the prediction of chemoresistance and subsequent suitability for DNMTi therapy could be informed by sampling OC patient's plasma cell-free tumor DNA (cfDNA) for specific methylation-based biomarkers [22].

Consistent with previous studies [23,24], we found the surgical debulking R0 in chemoresistant patients is significantly less than chemosensitive. D. Reyes et al. reported that the methylation pattern is different between patients with optimal and suboptimal surgical outcomes [24]. This epigenetic alteration may result in tumors behave more aggressively and therefore more likely to recur or less likely to be completely cytoreduced during surgery. Cardillo et al. used tumor genomics to create prediction models, which would predict an optimal or complete cytoreduction prior to entering the operating room [23]. Currently, there are no validated clinically relevant markers for chemoresistance in ovarian cancer available. The majority of previous attempts to define predictors of chemoresistance in ovarian cancer have been limited by a small number of patients, a mixture of histological types and stages, and a lack of validation in independent datasets. One of the more successful efforts involved the use of serum markers, including kallikreins and CA125. The AUC of these prediction models ranges from 75% to 85% [25,26]. The study developed a chemoresistance risk model using 43 candidate DMCs, which showed improved predictive ability for chemoresistance in EOC (AUC = 76.2%). The AUC of the risk model based on the Illumina 450K was better than that of the Illumina 27K. In the future, chips with higher coverage, such as Illumina 850K or genome-wide methylation analysis, should be used to promote the model's effectiveness.

Among the candidate DMCs, the methylations of cg08872590 and cg14739437 located in the gene body of LRRC24 were significantly related to increasing the risk of chemoresistance in EOC. While the upregulation of LRRC24 expression may lead to a poor prognosis. The methylation of cg15362155 located in the promoter of SCGB1D4 showed a significant impact in reducing the risk of chemoresistance. While the expression of SCGB1D4 may increase prognosis. However, the expression of LRRC24 and SCGB1D4 showed no difference between chemoresistant and chemosensitive patients. It is reported that methylation of circulating DNA can be detected in the serum [27]. Methylation of cg08872590, cg14739437 and cg15362155 may serve as predictive markers for predicting chemoresistance and prognosis in patients. However, further research is needed to validate these findings.

4.2. Corresponding DMGs of candidate DMCs

In the RNA sequencing transcriptomics data of TCGA ovarian cancer samples, further analysis was conducted on the 47 genes corresponding to the 51 candidate DMCs to investigate their potential association with chemoresistance. We identified 13 DMGs between chemosensitive and chemoresistant samples. The expression of DMGs was primarily negatively correlated with the methylation levels of corresponding DMCs. This is consistent with previous studies, indicating that the hypermethylation of CpGs leads to gene silencing, while hypomethylation usually leads to gene expression [7].

Heat shock proteins (HSPs) constitute a group of proteins that are involved in the reversal or inhibition ofthe denaturation or unfolding of cellular proteins in response to stress or elevated temperature. The HSPA family of HSPs, also known as the HSP70 family, has been reported to be associated with tumor progression and poor prognosis in specific cancer types, such as ovarian cancer [28]. HSPA1A protects tumor cells from oxidative stress, inflammatory cytokines, hypoxia, and other stresses [29]. It also involve in promoting tumor cell proliferation, metastasis, and invasion [30]. Hypomethylation of the HSPA1A promoter leads to increased expression of HSPA1A, which was associated with poor survival outcomes [31]. We found HSPA1A were significantly negatively correlated with corresponding hypermethylated cg12883479, which is located in the promoter region. In the tissue array utilized in this study, immunohistochemistry showed that HSPA1A was expressed both in the nucleus and cytoplasm. No statistically significant difference was observed between chemoresistant and chemosensitive EOC tissue. Consequently, we hypothesized that HSPA1A does not have a significant correlation with chemoresistance in EOC. Nevertheless, cg12883479 shows promise in epigenetic research related to HSPA1A.

The basement membrane (BM) is a planar extracellular matrix that is associated with cells and is situated within or around the majority of tissues. BM provide structural support, barrier functions, and signalling platforms for organizations [32]. Type IV collagen provides tensile strength to BM, allowing BM to structurally support tissues and resist mechanical forces [33]. The two main receptors for type IV collagen are integrin and the discoidin domain receptor (DDR). DDR2, one of the two DDR genes, plays a role in promoting attachment at the tissue linkage site in utse and seam cells [34]. Several studies have demonstrated the critical role of DDR2 in breast

cancer progression and metastasis, both in tumor cells and stromal cells [35]. Our study revealed a significant negative correlation between the expression of DDR2 and the corresponding hypomethylated cg23028772, which is located in the promoter region of the DDR2 gene. The expression of DDR2 was significantly higher in chemoresistant ovarian tissue compared to chemosensitive tissue. This suggests that hypomethylation of the DDR2 promoter may increase its expression, which is related to the development of chemotherapy resistance.

The opioid-binding protein cell adhesion molecule-like (OPCML) gene has demonstrated tumor-suppressor function in EOC both in vitro and in vivo [36]. According to a report, the methylation of OPCML is significantly higher in cell-free DNA extracted from the serum of early-stage ovarian carcinoma patients compared to healthy people [37]. Recent research on OPCML protein suggests that OPCML has potential as an anti-cancer therapy [36]. However, our study showed that OPCML expression was higher in chemoresistant tissue. OPCML exhibited a positive correlation with the corresponding DMC cg05035315, which is located within the gene body. This suggests that anticancer drugs related to OPCML may not be effective in patients with chemoresistance. However, cg05035315 is valuable for epigenetic studies related to OPCML and might be a specific methylation-based biomarkers for OPCML-relate therapy.

4.3. Limitations

This study's limitations should be noted. Firstly, the methods for screening the biomarkers were based on the statistical method rather than the biological experiment. Additionally, no experiments such as pyrosequencing were conducted to validate the methylation levels of the marker genes. Thirdly, further validation in prospective studies and multicenter clinical trials is needed. Chips with higher coverage like Illumina 850K could be used to promote the chemoresistance risk model effectiveness.

5. Conclusions

Our study suggests that hypomethylated CpGs may play a significant impact on the EOC chemoresistance. Some DMCs have shown considerable potential in predicting chemoresistance. The epigenetic modification of DDR2 may have a crucial role in the development of chemoresistance in EOC. The regulatory mechanism of DNA methylation in the development of chemoresistance in ovarian cancer is complex and diverse. Our study offers new avenues for future research.

CRediT authorship contribution statement

Changling Duan: Writing – original draft, Visualization, Project administration, Methodology, Formal analysis, Data curation, Conceptualization. **Zhongxin Yan:** Writing – review & editing, Writing – original draft, Visualization. **Cailiang Wu:** Writing – review & editing, Data curation. **Xuexin Zhou:** Writing – review & editing. **Wei Bao:** Writing – review & editing, Methodology, Funding acquisition, Conceptualization.

Declaration of competing interest

The authors declare that they have no known competing financial interests or personal relationships that could have appeared to influence the work reported in this paper.

Acknowledgements

We thank Dr. Jianming Zeng(University of Macau), and all the members of his bioinformatics team, biotrainee, for generously sharing their experience and codes. This study was funded by the National Natural Science Foundation of China (81972425), the National Natural Science Foundation of Shanghai (20ZR1444200), and the Clinical Project of Shanghai Municipal Health Commission (202240217).

Appendix A. Supplementary data

Supplementary data to this article can be found online at https://doi.org/10.1016/j.heliyon.2024.e27212.

Abbreviations

AUC	Area Under The Curve
BM	Basement Membrane
cfDNA	cell-free tumor DNA
CpGs	CpG Islands
DDR	Discoidin Domain Receptor
DNMTi	DNA Methyltransferase Inhibitors
DMCs	Different Methylated CpG Sites
DMGs	Different Methylated Gene Symbols
DMRs	Different Methylation Regions

EOC Epithelial Ovarian Cancer
GEO Gene Expression Omnibus
GO Gene Ontology
HSPs Heat Shock Proteins
Illumina 27K Illumina HumanMethylation27 BeadChip
Illumina 450K Illumina HumanMethylation450 BeadChip
KEGG Kyoto Encyclopedia of Genes and Genomes
OD Optical Density
OPCML Opioid-binding Protein Cell Adhesion Molecule-like
OS Overall Survival
TCGA The Cancer Genome Atla

References

[1] J.A. Doherty, L.C. Peres, C. Wang, G.P. Way, C.S. Greene, J.M. Schildkraut, Challenges and opportunities in studying the epidemiology of ovarian cancer subtypes, Curr Epidemiol Rep 4 (3) (2017) 211–220, https://doi.org/10.1007/s40471-017-0115-y.
[2] J. Prat, Ovarian carcinomas: five distinct diseases with different origins, genetic alterations, and clinicopathological features, Virchows Arch. 460 (3) (2012) 237–249, https://doi.org/10.1007/s00428-012-1203-5.
[3] M. Martín-Cameán, E. Delgado-Sánchez, A. Piñera, M.D. Diestro, J. De Santiago, I. Zapardiel, The role of surgery in advanced epithelial ovarian cancer, Ecancermedicalscience 10 (2016) 666, https://doi.org/10.3332/ecancer.2016.666.
[4] M.J. Piccart, K. Bertelsen, K. James, et al., Randomized intergroup trial of cisplatin-paclitaxel versus cisplatin-cyclophosphamide in women with advanced epithelial ovarian cancer: three-year results, J. Natl. Cancer Inst. 92 (9) (2000) 699–708, https://doi.org/10.1093/jnci/92.9.699.
[5] M. Timmermans, G.S. Sonke, K.K. Van de Vijver, M.A. van der Aa, R.F.P.M. Kruitwagen, No improvement in long-term survival for epithelial ovarian cancer patients: a population-based study between 1989 and 2014 in The Netherlands, Eur. J. Cancer 88 (2018) 31–37, https://doi.org/10.1016/j.ejca.2017.10.030.
[6] E. Papakonstantinou, G. Androutsopoulos, S. Logotheti, G. Adonakis, I. Maroulis, V. Tzelepi, DNA methylation in epithelial ovarian cancer: current data and future perspectives, CMP 14 (6) (2021) 1013–1027, https://doi.org/10.2174/1874467213666200810141858.
[7] Q.W. Chen, X.Y. Zhu, Y.Y. Li, Z.Q. Meng, Epigenetic regulation and cancer, Oncol. Rep. 31 (2) (2014) 523–532, https://doi.org/10.3892/or.2013.2913 (review).
[8] C. Zeller, W. Dai, N.L. Steele, et al., Candidate DNA methylation drivers of acquired cisplatin resistance in ovarian cancer identified by methylome and expression profiling, Oncogene 31 (42) (2012) 4567–4576, https://doi.org/10.1038/onc.2011.611.
[9] Y. Pan, G. Liu, F. Zhou, B. Su, Y. Li, DNA methylation profiles in cancer diagnosis and therapeutics, Clin. Exp. Med. 18 (1) (2018) 1–14, https://doi.org/10.1007/s10238-017-0467-0.
[10] R.P. Talens, D.I. Boomsma, E.W. Tobi, et al., Variation, patterns, and temporal stability of DNA methylation: considerations for epigenetic epidemiology, Faseb. J. 24 (9) (2010) 3135–3144, https://doi.org/10.1096/fj.09-150490.
[11] A.M. Oza, U.A. Matulonis, A. Alvarez Secord, et al., A randomized phase II trial of epigenetic priming with guadecitabine and carboplatin in platinum-resistant, recurrent ovarian cancer, Clin. Cancer Res. 26 (5) (2020) 1009–1016, https://doi.org/10.1158/1078-0432.CCR-19-1638.
[12] D. Matei, S. Ghamande, L. Roman, et al., A phase I clinical trial of guadecitabine and carboplatin in platinum-resistant, recurrent ovarian cancer: clinical, pharmacokinetic, and pharmacodynamic analyses, Clin. Cancer Res. 24 (10) (2018) 2285–2293, https://doi.org/10.1158/1078-0432.CCR-17-3055.
[13] C.A. Barton, N.F. Hacker, S.J. Clark, P.M. O'Brien, DNA methylation changes in ovarian cancer: implications for early diagnosis, prognosis and treatment, Gynecol. Oncol. 109 (1) (2008) 129–139, https://doi.org/10.1016/j.ygyno.2007.12.017.
[14] E. Papakonstantinou, G. Androutsopoulos, S. Logotheti, G. Adonakis, I. Maroulis, V. Tzelepi, DNA methylation in epithelial ovarian cancer: current data and future perspectives, CMP 14 (6) (2021) 1013–1027, https://doi.org/10.2174/1874467213666200810141858.
[15] A.M. Patch, E.L. Christie, D. Etemadmoghadam, et al., Whole-genome characterization of chemoresistant ovarian cancer, Nature 521 (7553) (2015) 489–494, https://doi.org/10.1038/nature14410.
[16] J. Zhang, Y. Chen, X. Chen, et al., Deubiquitinase USP35 restrains STING-mediated interferon signaling in ovarian cancer, Cell Death Differ. 28 (1) (2021) 139–155, https://doi.org/10.1038/s41418-020-0588-y.
[17] X. Yang, H. Han, D.D. De Carvalho, F.D. Lay, P.A. Jones, G. Liang, Gene body methylation can alter gene expression and is a therapeutic target in cancer, Cancer Cell 26 (4) (2014) 577–590, https://doi.org/10.1016/j.ccr.2014.07.028.
[18] C. Zeller, W. Dai, N.L. Steele, et al., Candidate DNA methylation drivers of acquired cisplatin resistance in ovarian cancer identified by methylome and expression profiling, Oncogene 31 (42) (2012) 4567–4576, https://doi.org/10.1038/onc.2011.611.
[19] D. Matei, F. Fang, C. Shen, et al., Epigenetic resensitization to platinum in ovarian cancer, Cancer Res. 72 (9) (2012) 2197–2205, https://doi.org/10.1158/0008-5472.CAN-11-3909.
[20] Y. Wang, H. Cardenas, F. Fang, et al., Epigenetic targeting of ovarian cancer stem cells, Cancer Res. 74 (17) (2014) 4922–4936, https://doi.org/10.1158/0008-5472.CAN-14-1022.
[21] S. Nunna, R. Reinhardt, S. Ragozin, A. Jeltsch, Targeted methylation of the epithelial cell adhesion molecule (EpCAM) promoter to silence its expression in ovarian cancer cells, PLoS One 9 (1) (2014) e87703, https://doi.org/10.1371/journal.pone.0087703.
[22] K. Song, M. Artibani, The role of DNA methylation in ovarian cancer chemoresistance: a narrative review, Health Science Reports 6 (5) (2023) e1235, https://doi.org/10.1002/hsr2.1235.
[23] N. Cardillo, E.J. Devor, S. Pedra Nobre, et al., Integrated clinical and genomic models to predict optimal cytoreduction in high-grade serous ovarian cancer, Cancers 14 (14) (2022) 3554, https://doi.org/10.3390/cancers14143554.
[24] H.D. Reyes, E.J. Devor, A. Warrier, et al., 【GSE133556】Differential DNA methylation in high-grade serous ovarian cancer (HGSOC) is associated with tumor behavior, Sci. Rep. 9 (1) (2019) 17996, https://doi.org/10.1038/s41598-019-54401-w.
[25] K. Oikonomopoulou, L. Li, Y. Zheng, et al., Prediction of ovarian cancer prognosis and response to chemotherapy by a serum-based multiparametric biomarker panel, Br. J. Cancer 99 (7) (2008) 1103–1113, https://doi.org/10.1038/sj.bjc.6604630.
[26] Y. Zheng, D. Katsaros, S.J.C. Shan, et al., A multiparametric panel for ovarian cancer diagnosis, prognosis, and response to chemotherapy, Clin. Cancer Res. 13 (23) (2007) 6984–6992, https://doi.org/10.1158/1078-0432.CCR-07-1409.
[27] M. Widschwendter, M. Zikan, B. Wahl, et al., The potential of circulating tumor DNA methylation analysis for the early detection and management of ovarian cancer, Genome Med. 9 (1) (2017) 116, https://doi.org/10.1186/s13073-017-0500-7. Published 2017 Dec 22.
[28] W.P. De Andrade, L. Da Conceição Braga, N.G. Gonçales, L.M. Silva, A.L. Da Silva Filho, HSPA1A, HSPA1L and TRAP1 heat shock genes may be associated with prognosis in ovarian epithelial cancer, Oncol. Lett. 19 (1) (2020) 359–367, https://doi.org/10.3892/ol.2019.11095.
[29] C. Garrido, M. Brunet, C. Didelot, Y. Zermati, E. Schmitt, G. Kroemer, Heat shock proteins 27 and 70: anti-apoptotic proteins with tumorigenic properties, Cell Cycle 5 (22) (2006) 2592–2601, https://doi.org/10.4161/cc.5.22.3448.

[30] Q. Chen, K. Wu, X. Qin, Y. Yu, X. Wang, K. Wei, LASP1 promotes proliferation, metastasis, invasion in head and neck squamous cell carcinoma and through direct interaction with HSPA1A, J. Cell Mol. Med. 24 (2) (2020) 1626–1639, https://doi.org/10.1111/jcmm.14854.
[31] Y. Guan, X. Zhu, J. Liang, M. Wei, S. Huang, X. Pan, Upregulation of HSPA1A/HSPA1B/HSPA7 and downregulation of HSPA9 were related to poor survival in colon cancer, Front. Oncol. 11 (2021). https://www.frontiersin.org/articles/10.3389/fonc.2021.749673. (Accessed 6 June 2023).
[32] M.A. Morrissey, D.R. Sherwood, An active role for basement membrane assembly and modification in tissue sculpting, J. Cell Sci. 128 (9) (2015) 1661–1668, https://doi.org/10.1242/jcs.168021.
[33] A.L. Fidler, S.P. Boudko, A. Rokas, B.G. Hudson, The triple helix of collagens - an ancient protein structure that enabled animal multicellularity and tissue evolution, J. Cell Sci. 131 (7) (2018) jcs203950, https://doi.org/10.1242/jcs.203950. . Published 2018 Apr 9.
[34] K. Park, R. Jayadev, S.G. Payne, et al., Reciprocal discoidin domain receptor signaling strengthens integrin adhesion to connect adjacent tissues, Elife 12 (2023) RP87037, https://doi.org/10.7554/eLife.87037.
[35] C.C. Lin, W.H. Yang, Y.T. Lin, et al., DDR2 upregulation confers ferroptosis susceptibility of recurrent breast tumors through the Hippo pathway, Oncogene 40 (11) (2021) 2018–2034, https://doi.org/10.1038/s41388-021-01676-x.
[36] Y. Shao, J. Kong, H. Xu, et al., OPCML methylation and the risk of ovarian cancer: a meta and bioinformatics analysis, Front. Cell Dev. Biol. 9 (2021) 570898, https://doi.org/10.3389/fcell.2021.570898.
[37] B. Wang, L. Yu, X. Luo, et al., Detection of OPCML methylation, a possible epigenetic marker, from free serum circulating DNA to improve the diagnosis of early-stage ovarian epithelial cancer, Oncol. Lett. 14 (1) (2017) 217–223, https://doi.org/10.3892/ol.2017.6111.